AFRL-VS-TR-1999-1536

Small On-Board Environmental Diagnostic Sensors Package (SOBEDS)

Robert H. Redus
Alan C. Huber
Phil D'Entremont
John O. McGarity
David J. Sperry
Alan Donkin
Marilyn R. Oberhardt
John A. Pantazis
Bronislaw K. Dichter

AMPTEK, Inc.
6 DeAngelo Drive
Bedford, MA 01730

14 February 2000

Scientific Report No. 3

AIR FORCE RESEARCH LABORATORY
Space Vehicles Directorate
29 Randolph Rd
AIR FORCE MATERIEL COMMAND
Hanscom AFB, MA 01731-3010

This Technical Report has been reviewed and is approved for publication.

Donald Brautigam
Contract Manager

Gregory P.Ginet, Chief
Space Hazards Branch

This report has been reviewed by the ESC Public Affairs Office (PA) and is releasable to the National Technical Information Service.

Qualified requestors may obtain additional copies from the Defense Technical Information Center (DTIC). All others should apply to the National Technical Information Service (NTIS).

If your address has changed, if you wish to be removed from the mailing list, of if the address is no longer employed by your organization, please notify AFRL/VSOS-IMA, 29 Randolph Rd., Hanscom AFB, MA 01731-3010. This will assist us in maintaining a current mailing list.

Do not return copies of this report unless contractual obligations or notices on a specific document require that it be returned.

REPORT DOCUMENTATION PAGE

Form Approved
OMB No. 0704-0188

1. AGENCY USE ONLY *(Leave blank)*	2. REPORT DATE	3. REPORT TYPE AND DATES COVERED
	05/05/99	Scientific No.3

4. TITLE AND SUBTITLE

Small On-Board Environmental Diagnostics Sensor Package (SOBEDS)

5. FUNDING NUMBERS

PE 63410F
PR 2822 TA GC WU AM

Contract F19628-95-C-0227

6. AUTHOR(S)

Robert H. Redus, John O. McGarity, Marilyn R. Oberhardt
Alan C. Huber, David J. Sperry, John A. Pantazis
Phil D'Entremont, Alan Donkin, Bronislaw K. Dichter

7. PERFORMING ORGANIZATION NAME(S) AND ADDRESS(ES)

AMPTEK, Inc.
6 De Angelo Drive
Bedford, MA 01730

8. PERFORMING ORGANIZATION REPORT NUMBER

9. SPONSORING/MONITORING AGENCY NAME(S) AND ADDRESS(ES)

Air Force Research Laboratory
29 Randolph Road
Hanscom AFB, MA 01731-3010

Contract Manager: Don Brautigam/VSBS

10. SPONSORING/MONITORING AGENCY REPORT NUMBER

AFRL-VS-TR-1999-1536

11. SUPPLEMENTARY NOTES

12a. DISTRIBUTION AVAILABILITY STATEMENT

Approved for public release; distribution unlimited

12b. DISTRIBUTION CODE

13. ABSTRACT *(Maximum 200 words)*

The Small On-Board Environmental Sensors Package (SOBEDS) is a suite of spacecraft instruments designed to measure ionizing radiation in the near-Earth space environment. The purpose of data gathered by the SOBEDS instrument is to improve the understanding of the Earth's radiation belts and the effect of ionizing radiation on Air Force space systems. This report is concerned with the experimental and computational effort in the design of the High Energy Proton (HEP) sensor for the SOBEDS suite. HEP is designed to measure the differential energy fluxes of protons with energies between 25 and 300 MeV. This report also covers design and development of the LEPDOS instruments.

14. SUBJECT TERMS

Spacecraft Radiation Measurement, Electrons, Protons, Dosimetry

15. NUMBER OF PAGES

26

16. PRICE CODE

17. SECURITY CLASSIFICATION OF REPORT	18. SECURITY CLASSIFICATION OF THIS PAGE	19. SECURITY CLASSIFICATION OF ABSTRACT	20. LIMITATION OF ABSTRACT
Unclassified	Unclassified	Unclassified	SAR

Table of Contents

Figures

Tables

1 INTRODUCTION

This report contains the summary of the scientific and engineering work performed as part of the development of the High Energy Proton instrument (HEP) and of the Low Energy Particle and Dosimetry instrument (LEPDOS). These instruments are part of the SOBEDS suite of instruments being developed by Amptek, Inc. The purpose of the HEP instrument is to measure the energy spectrum of energetic protons, specifically to obtain a differential spectrum for $25 \leq E \leq 440$ MeV and integral counts for E>440 MeV. The purpose of the LEPDOS instrument is to measure: 1) the lower energy protons and electrons which may cause spacecraft anomalies, specifically protons from 0.7 to 80 MeV and electrons from 0.5 to >250 keV, 2) the dose and dose rate experienced by spacecraft electronics, 3) particles causing single event effects, and 4) to provide real-time warnings to spacecraft and operators of environmental conditions likely to cause anomalies, such as surface charging and deep dielectric charging.

During the third year of the SOBEDS contract, the primary technical effort on HEP has been devoted to the design, manufacture, and testing of the protoflight HEP sensor head. A key element of the design process was calculation of the response of the instrument to off-axis protons and to nuclear interactions. Another key element was the design of a rugged, compact mechanical assembly and the design of low power, low noise analog electronics. A protoflight sensor was fabricated and tested with radioactive sources at Amptek, Inc. and with proton beams at two accelerators, the Harvard Cyclotron (HCL) and the Alternating Gradient Synchrotron (AGS) at the Brookhaven National Laboratory (BNL).

The primary technical effort on LEPDOS in this third year of the SOBEDS contract has been devoted to the design, fabrication, and testing of two flight LEPDOS instruments, and also to the design of an engineering model LEPDOS instrument which includes an electrostatic analyzer (ESA) to measure electrons with energy below the threshold of the standard LEPDOS sensors.

2 HEP FLIGHT INSTRUMENT DESIGN AND DEVELOPMENT

2.1 INSTRUMENT CONCEPT

The measurement of high energy protons represents a challenge due to their large range in matter (300 MeV protons have a range of 24 cm in aluminum) and to the fact that the rate of energy loss in matter is low and varies slowly with energy above 150 MeV. This measurement is particularly difficult in space, where a nearly isotropic distribution of penetrating protons exists, and where minimal shielding mass can be flown.

The HEP instrument uses a combination of detectors, including two scintillators, a veto scintillator, and four solid state detectors, to identify in-aperture protons and to measure their energy. The detectors have been arranged to permit a clean measurement of the energy of in-aperture protons with energies between 20 and 440 MeV in the presence of an intense flux of out-of-aperture high energy protons. A conceptual drawing of the HEP sensor is shown in Figure 1.

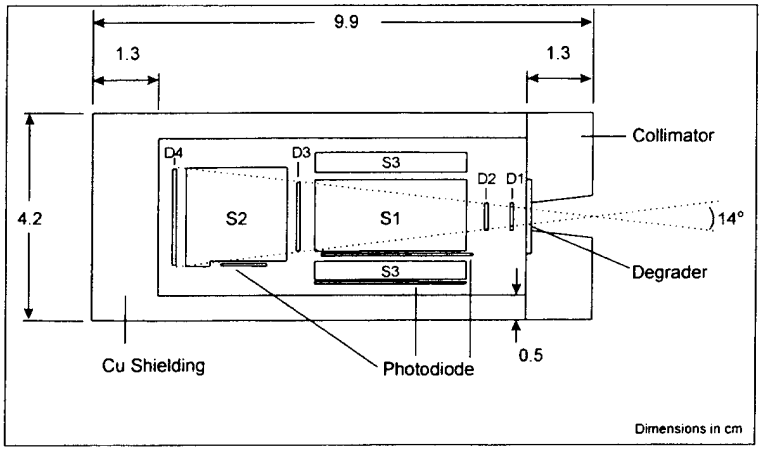

Figure 1. Conceptual drawing of the HEP sensor geometry, showing the S1 and S2 GSO scintillators, the D1-D4 Si PIPS diodes, the S3 veto scintillator, and shielding and collimation.

Figures 2 and 3 show calculated energy depositions in the detectors. In-aperture proton events will be classified into three general types:

Type A: proton traverses D1, D2 and stops in S1,
Type B: proton traverses D1, D2, S1, D3 and stops in S2,
Type C: proton traverses D1, D2, S1, D3, S2 and D4.

These in-aperture event types are caused by protons with different kinetic energies. Protons with energies between the degrader threshold of 20 MeV and 120 MeV will stop in S1 and produce Type A events. Type B events are caused by protons with energies between the Type A maximum of 120 MeV and 175 MeV. Type C events are due to protons with energies above 175 MeV. Differential energy measurements for Type C events are made up to a proton energy of 440 MeV. Incident energies above 440 MeV will produce smaller energy depositions (S1 and S2 < 40 MeV) and be measured in an integral channel. Note that both front and rear entry protons in the highest energy channels will be detected as Type C events.

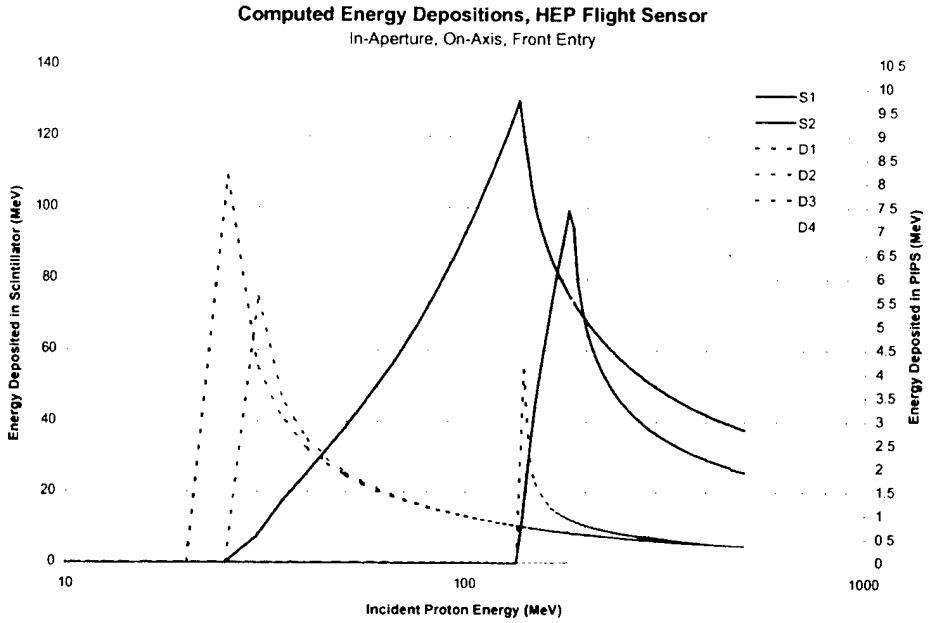

Figure 2. Plot showing energy deposited in the six on-axis detectors as a function of incident proton energy, computed using the Janni models. The combination of the pattern of D detectors which are triggered, along with the amount of energy deposited in S1 and S2, permits accurate measurement of the incident proton energy.

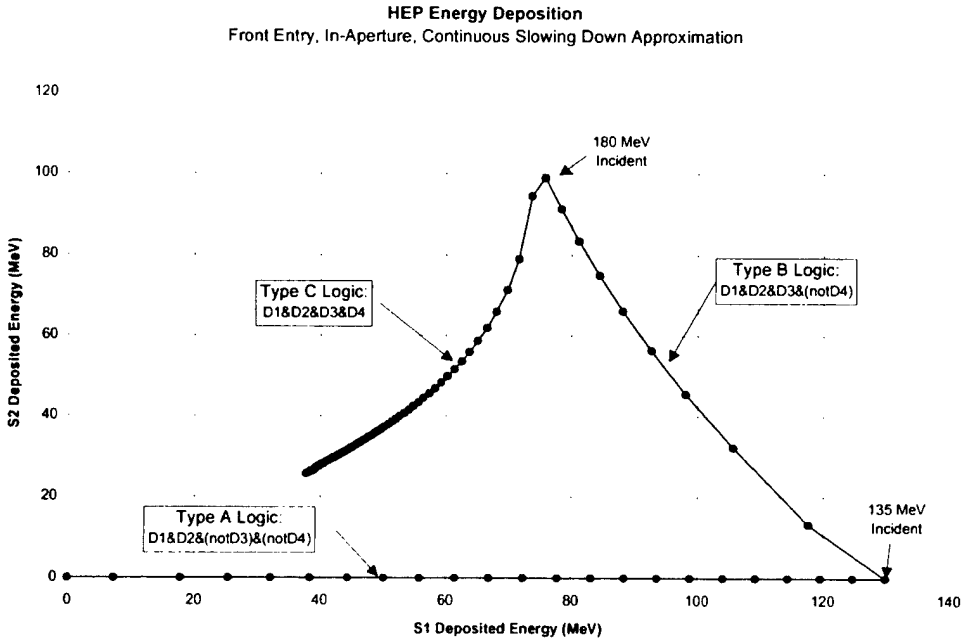

Figure 3. Plot showing the energy deposited in S2 versus S1, along with the PIPS detector logic, as a function of incident energy. This is the same data as is shown in figure 2.

In addition to the three primary event types (A,B, and C), there can be many other types. Those of interest include those caused by: 1) particles entering through the rear and passing through the aperture, 2) out-of-aperture protons penetrating the HEP collimator, 3) in-aperture protons undergoing nuclear interaction in HEP, and 4) random, accidental, simultaneous triggering of two or more detectors. These classes of events form the "background" which must be quantified to obtain an accurate knowledge of the incident spectrum. The HEP data processing system will be designed to make on-orbit measurements of these "background" event types, allowing correction factors to be determined for these events.

As discussed in the second annual report, in the first two years of this program an engineering model (EM) of the HEP sensor head was manufactured for the purpose of testing the key hardware components and data handling algorithms intended for use with the flight instrument. The EM sensor head did not include any internal electronics. All signal processing and data acquisition were performed by external electronic modules, both custom designed and commercial NIM electronics. Using the EM, we performed extensive experimental and computational work to characterize the response of the HEP sensor head to protons. The overall agreement between experimental data and the calculation results was excellent, suggesting that the HEP sensor head simulations are accurate. We are now using results of the simulation work to further refine the sensor head design.

During the third year of the SOBEDS contract, the primary technical effort on HEP has been devoted to the design, manufacture, and testing of the protoflight HEP sensor head, using the results obtained previously with the EM. The protoflight sensor head is intended to be completely identical, in every way, to the flight sensor head. The protoflight unit was built first in order to validate the design, before the flight instrument is built.

2.2 INSTRUMENT OPERATION AND REQUIREMENTS

A crucial part of the design process has been definition of requirements and of the inputs and outputs, including the data telemetered to the ground, on-board processing, and operating modes. The requirements were defined in close coordination with AFRL personnel. There will be 22 primary energy channels, corresponding to the energy deposited by front entry protons. The approximate boundaries of these channels are shown in the table below.

Chan. No.	Energy Range (MeV)	Width (MeV)	Chan. No.	Energy Range (MeV)	Width (MeV)
1	< 30		12	110-120	10
2	30-35	5	13	120-140	20
3	35-40	5	14	140-160	20
4	40-45	5	15	160-180	20
5	45-50	5	16	180-200	20
6	50-60	5	17	200-230	30
7	60-70	10	18	230-260	30
8	70-80	10	19	260-300	40
9	80-90	10	20	300-360	60
10	90-100	10	21	360-440	80
11	100-110	10	22	> 440	

Table 1. Table of the approximate energy channels for front-entry, in-aperture protons.

To determine the energy of an incident proton, HEP will use both the pattern of PIPS detectors which are triggered and the amount of energy deposited in the scintillators. This combination is key to a valid measurement. For example, a 330 MeV proton should trigger all four PIPS detectors (D1, D2, D3, and D4), should not trigger S3, and should deposit a certain amount of energy in S1 and a certain amount in S2 (defined by a certain region in the S1S2 plane, along the curve shown in Figure 3). Only if all these conditions are met is there a valid, in-aperture proton corresponding to channel 20.

In addition to the counts in these 22 energy channels, it will be necessary to return measurements of the "background" events mentioned previously. As discussed later in this report, these background events produce signatures in either the S1S2 plane or in the PIPS detectors which differ from those due to the front-entry protons. The HEP electronics will measure the fluxes of these background events.

To carry out this measurement, additional regions in the S1S2 plane will be defined which correspond to the pattern of deposition due to background events. This corresponds to additional "channels". HEP will have a total of 48 channels, each corresponding to a region in the S1S2 plane, although not necessarily to a unique incident energy. To provide maximum flexibility, these channels can be altered during flight. We will also measure the number of particles in each of the 48 channels not only for the PIPS pattern expected for in-aperture protons, but for other PIPS patterns as well. HEP will contain six logic masks, each corresponding to a pattern of PIPS triggers, each of which can be set during flight.

The primary HEP telemetry output will consist of six different 24 channel spectra. Each spectrum reflects counts in a selected logic mask and S1S2 values corresponding to either channels 1-24 (nominal, front-entry) or 25-48 (rear entry, nuclear events, etc.) The set of logic masks and channels can be altered during flight. These data will be integrated over an interval which can be set to 0.1-10 seconds before instrument delivery. In addition to these data, HEP will return the raw count rates in each of the seven detectors and for each of the six logic masks.

A block diagram of the HEP electronic design is given in Figure 4. Each of the seven detectors has an analog preamplifier and shaping amplifier. The PIPS detector analog signals are sent to comparators, which trigger the coincidence circuitry and perform a crude pulse-height analysis. The S3 signal goes to a timing discriminator, which triggers the coincidence circuitry. The S1 and S2 scintillator outputs go to an analog to digital converter.

The digital signal processing (DSP) portion of the circuitry uses the pattern of detectors which were triggered, determined by the coincidence logic, and the amount of energy deposited in the S1 and S2 scintillators, to determine if a particular event is valid. If so, then the DPU increments the appropriate spectrum counter. The coincidence logic determines if the pattern of triggered detectors matches that in one of the six logic masks The S1S2 lookup table relates the S1S2 deposited energies to the 48 "energy" channels. Both the logic masks and the S1S2 lookup table can be changed during flight.

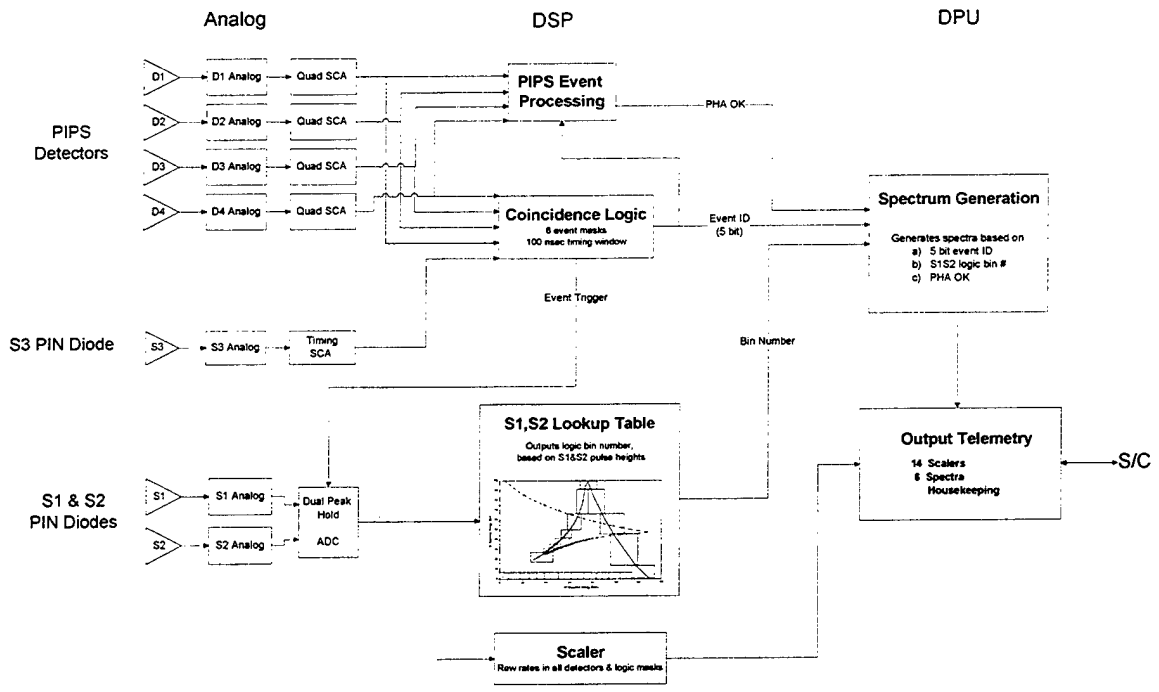

Figure 4. Block diagram of the HEP analog and digital electronics.

Small size, light weight, and low power are important aspects of the HEP design. HEP will consist of two different boxes, a sensor head and an electronics box, as discussed below. Using two boxes provides additional flexibility in mounting HEP on small spacecraft. The total mass of HEP is not to exceed 2.6 kg. The total power consumption is not to exceed 6 watts. The telemetry package size is not to exceed 350 bytes. The data can be updated at intervals between 1 and 10 seconds, set before delivery. All of the electronics are radiation hardened to at least 100 krad.

2.3 SENSOR DESIGN AND FABRICATION

The HEP instrument includes seven different radiation detectors, listed below. A complete set of sensors was obtained for use in the protoflight instrument.

D1: 700 μm thick, 0.25 cm^2 area PIPS detector
D2: 700 μm thick, 0.25 cm^2 area PIPS detector
S1: GSO scintillator, 3 cm long by 1.2 cm dia
D3: 700 μm thick, 1.50 cm^2 area PIPS detector
S2: GSO scintillator, 2 cm long by 2 cm dia
D4: 700 μm thick, 3.00 cm^2 area PIPS detector
S3: Plastic scintillator hollow cylinder, surrounding D1, D2, and S1

The four PIPS detectors are commercially available silicon diodes, ion-implanted devices with demonstrated good performance and excellent ruggedness. They were obtained from Canberra, Inc., and used as provided.

The S1 and S2 scintillators are made from Gd_2SiO_5 (GSO), because of its unique combination of high stopping power, high light output, fast decay time, and manufacturability, as

discussed in the previous annual report. The S3 veto scintillator is made from a scintillating plastic, BC-428, which has somewhat lower light output than GSO but a much faster decay time. The design of the flight sensors included detailed design of the sensor geometry, selection of the photodetector to read out the scintillators, and the design of optical reflectors to maximize the optical signal. A critical consideration in the design was the need to minimize the diameter of the S1 and S3 stack, in order to minimize the mass of the shielding and to minimize the number of false veto events due to protons incident on S3.

The lengths of the S1 and S2 scintillators were chosen to maximize the total energy deposition within HEP, given the desired angular acceptance cone (7° half-angle) and the diameters of the D3 and D4 detectors, limited to commercially available values. A length of 3 cm for S1 and 2 cm for S2 was optimum and leads to a signal amplitude of 30 MeV and 20 MeV, respectively, for minimum ionizing particles. The S3 geometry is a trade-off: a thicker scintillator gives a large signal, but the larger area leads to a higher false veto rate. A thickness of 5 mm, with a minimum energy deposition of 2.5 MeV for protons of interest, was chosen.

We have chosen to use photodiodes (PD) for optical readout, instead of the more conventional photomultiplier tubes (PMT). PMTs have less noise, but have several significant practical disadvantages. Moreover, data taken with the EM show that the additional noise of the PD is negligible compared with the scintillator's intrinsic resolution. Data taken with the EM at HCL and BNL showed that the intrinsic resolution of a 2 cm GSO scintillator, for minimum ionizing particles and a PMT readout, is about 3 MeV. The PD has an electronic noise of <0.5 MeV, for a total peak broadening of 3.04 MeV. The PMTs practical disadvantages include 1) its large size, which requires either additional shielding mass or decreased shielding, 2) the necessity for high voltage, 3) higher power consumption, and 4) sensitivity to magnetic fields. The PD was clearly a superior choice given the practical considerations of space instrumentation and the relatively large optical signals generated in the scintillator by energetic protons.

In order to obtain a good signal to noise ratio, it is critical that the maximum number of photons interact in the PD. This requires good optical coupling of the PD to the scintillator, and a good optical reflector around the scintillator. To obtain good optical coupling, the scintillators were fabricated with a flat surface onto which the PD could be coupled, as shown in Figure 5. The photodiodes, which are commercially available from Hamamatsu, Inc., were epoxied to the scintillators by Bicron, Inc., using space-flight qualified materials and procedures.

For any interaction in the scintillator, with photons emitted isotropically, there is only a small solid angle with photons directly incident on the PD. The scintillator must be surrounded by a reflective material, so that the photons may be reflected (sometimes many times) and still collected. The optical reflector chosen for use in HEP is Spectralon, a sintered Teflon with a reflectance exceeding 99% for optical wavelengths from 300 to 1800 nm. Each of the scintillators was surrounded by at least 1 mm of Spectralon, to obtain the necessary reflectance. Because S1 is surrounded by S3, there was concern of optical cross-talk between the two, so a metallic layer was inserted between the S1 and S3 optical reflectors. In tests at HCL, no optical cross-talk was observed. Figure 5 is a photo of the S1 and S3 scintillator stack, showing the flight scintillator, photodiodes, and Spectralon reflectors. A penny is shown for comparison. The outside diameter of the largest reflector is 3 cm. The tight geometry is clearly visible in this photo.

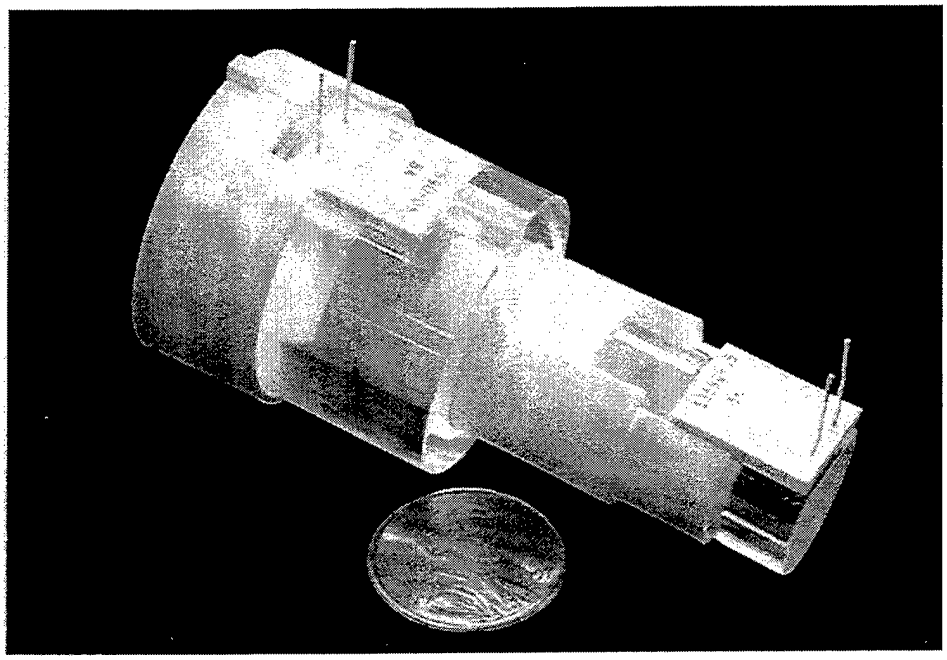

Figure 5. Photograph of the S1 and S3 sensor stack, showing the scintillators, photodiodes, and optical reflectors.

2.4 SENSOR HEAD MECHANICAL DESIGN AND FABRICATION

The HEP flight instrument will consist of two components, a sensor head and an electronics box. A drawing of the two components is shown in Figure 6. The sensor head will contain the seven sensors, with shielding, along with preamplifiers and amplifiers for each sensor. The electronics box will contain analog electronics, digital data processing electronics, the spacecraft interface, and the power supply. The instrument was divided into two boxes to provide maximum flexibility in mounting the instrument, since only the sensor head need be mounted on the exterior of the spacecraft. The cable between the two boxes can be up to one meter long.

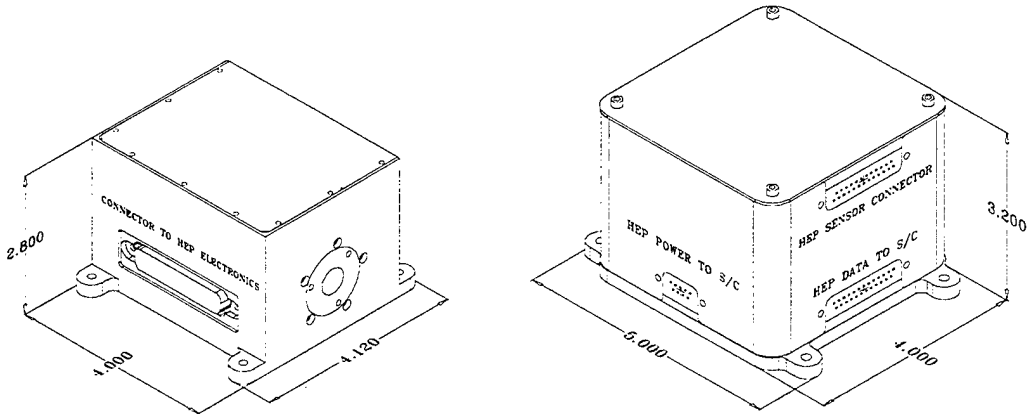

Figure 6. Preliminary drawings of the HEP sensor head (left) and electronics box (right).

The protoflight sensor head includes the seven sensors discussed above, along with mechanical hardware required to hold the detectors in place. These are mounted inside a copper

shield, 5 mm thick along the sides and 1.3 cm thick on the front and rear. The front is also coveredby 2.5 mm of tungsten. The minimum energy required to penetrate the shield is 60 MeV through the side, 130 MeV through the front, and 100 MeV through the rear. This keeps the maximum out-of-aperture count rates in the scintillator to an acceptable level. We used the AP8 model to compute that S3, at the peak of the proton radiation belt, will experience an out-of-aperture count rate of about 130,000 sec^{-1}, which leads to an acceptably low false veto rate given the 100 nsec timing window to be used. Additional shielding would lead to a significant weight penalty.

The front collimator was designed to minimize the effect of out-of-aperture protons, while permitting a clean measurement of all in-aperture type C protons. The collimator was fabricated from tungsten, which provides the highest possible stopping per unit volume. This is crucial for those out-of-aperture trajectories that have a short path length through the collimator: using tungsten stops as many of these protons as possible. The opening of the collimator was chosen so that no trajectory that passes through the D1 and D4 active areas will be degraded by the collimator. The tungsten extends over the entire front of the active portion of the instrument, to provide additional shielding.

The sensor head also includes the box, which holds the sensor stack and shielding, and also holds the preamplifier board, the sensor to electronics box connector, and a test input connector. The sensor stack and shielding are located at the bottom, so the center of mass is low. The complete sensor head was fabricated, and the protoflight unit assembled and used in the test and calibration described below. The total mass of the protoflight sensor head is 1.4 kg. The mass breakdown is shown in Table 2.

Detectors	175 g
Collimator	60 g
Shielding	685 g
Boards and Connectors	120 g
Sensor Head Box	415 g
Total	**1.45 kg**

Table 2. Sensor head mass

The mechanical design of the electronics box is very similar to that used in the LEPDOS instruments. It has the same footprint as LEPDOS, and the same power and I/O connectors. The HEP electronics box will be shorter than the LEPDOS box, since there are fewer boards. It will also have an additional connector, to connect with the sensor head.

2.5 Analog Electronic Design and Fabrication

In the most recent year, detailed design of the analog electronics was carried out. The protoflight preamplifier board was fabricated and tested, and has been used in the completed protoflight sensor head. A breadboard prototype of the amplifier board, which will be located in the electronics box, was fabricated and was used in the beam testing discussed below.

The four PIPS detectors use identical analog circuitry, shown in Figure 7. The detector output is passed to an A225 hybrid preamplifier and shaping amplifier. The fast timing output of the A225 is sent to an A275 hybrid amplifier with additional pulse shaping. The output of the

A275 is a fast analog signal, with a measured risetime of 75 nsec, a falltime of 300 nsec, and amplitude of about 1 V/MeV. These hybrids are located on the preamplifier board in the sensor head, so that relatively large signals are sent across the cable to the electronics box. In the electronic box, the A275 outputs go to 9405 hybrid comparators. The fast discriminator triggers the coincidence logic, while the quad discriminator outputs, which provide rough pulse height analysis, go to the PIPS PHA processing logic.

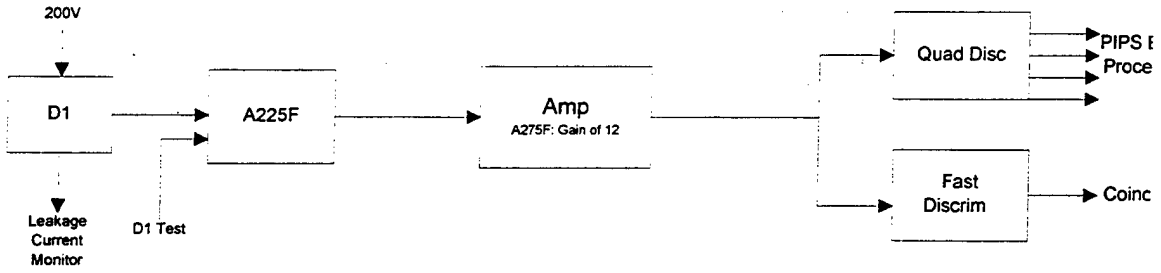

Figure 7. Design of analog electronics used with the four PIPS detectors.

The S1 and S2 scintillator outputs use identical analog circuits, shown in Figure 8. The output of the PIN diodes goes to an A250F hybrid charge sensitive preamplifier. The preamp output goes to a 5 pole pseudo-gaussian shaping amplifier, with a shaping time constant of 0.25 μsec, implemented using A275 hybrids. This shaping time was chosen as a trade-off between the electronic noise, which is reduced at longer shaping times, and pulse pile-up, which is reduced at shorter shaping times. The output of the shaping amplifier is sent to a circuit which captures and digitizes the peak amplitude. This will be used by the DSP circuitry, to determine in which of the 48 channels the count occurred. The digitization is initiated by the coincidence circuitry.

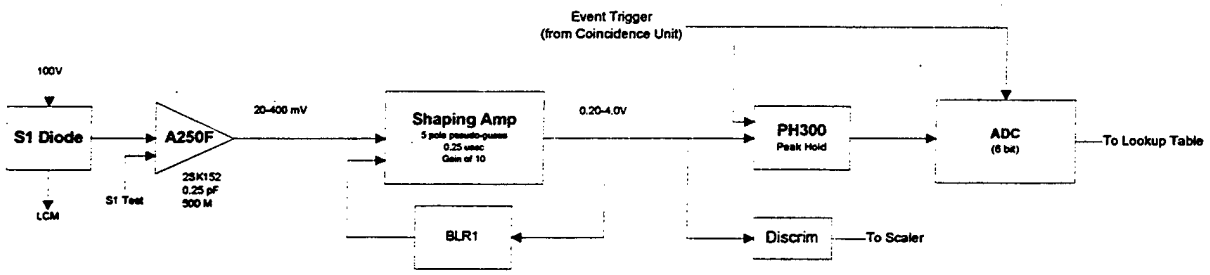

Figure 8. Design of analog electronics used with the S1 and S2 detectors.

The preamplifier and a portion of the shaping amplifier are located in the sensor head. A flight board with this portion was built and used in the testing. The rest of the shaping amplifier was implemented in a breadboard circuit, used in the tests below. In the current protoflight, an external CAMAC digitizer was used.

The S3 circuit is similar to the S1 and S2 circuits. It uses an A250F hybrid preamplifier and a pseudo-gaussian shaping amplifier, but with a 0.1 μsec shaping time constant, giving a pulse risetime of 200 nsec. However, the output is connected to a timing discriminator instead of a digitizer. A crossover timing discriminator was used, with a measured timing resolution of <20

nsec FWHM. Using a shorter shaping time increases the noise, which actually degrades the timing resolution, since the resolution of a crossover timing discriminator depends on noise.

2.6 DIGITAL ELECTRONICS DESIGN

The detailed design of the digital electronics in HEP was begun in this past year. The initial focus has been on developing the general architecture for the digital signal processing, and on designing the coincidence circuitry. The coincidence circuitry to obtain 100 nsec timing resolution is anticipated to represent a significant technical challenge, given the requirement of a 200 nsec risetime of the S3 signal, the need to recognize six simultaneous logic masks, the ability to alter masks, and the constraints on low power and radiation hardness. Because the rate of false vetoes and false positives depends upon the timing window, the timing window must be stable over the full range of temperatures and other environmental conditions expected.

Figure 9 shows a timing diagram illustrating the intended design. We are now beginning the detailed circuit design, recognizing that the details of the timing will doubtless change. The delays will be implemented using passive delay lines, which are reliable, stable, devices. The logic will be implemented using an FPGA. The design will be fully asynchronous, as is required given the timing of the events.

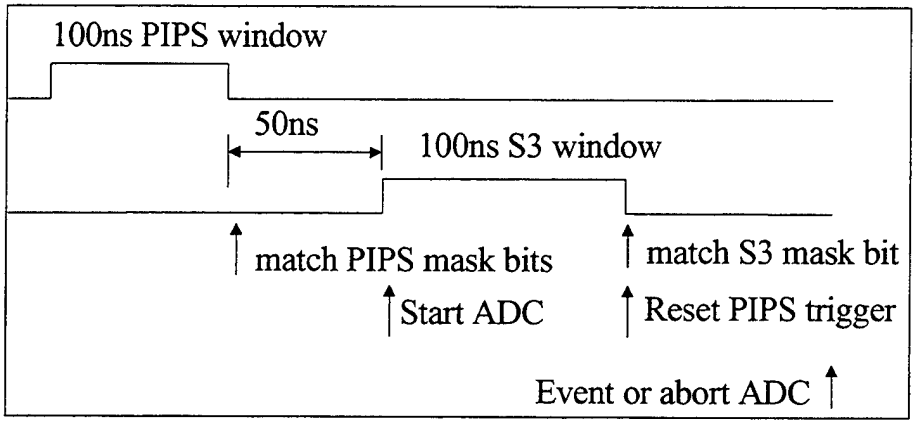

Figure 9. Timing diagram for the planned coincidence logic.

The four PIPS signals have a risetime of <75 nsec, while the S3 signal has a 200 nsec risetime. In order to obtain the required 100 nsec timing resolution, a two part coincidence circuit will be used. The anticipated timing diagram is illustrated in Figure 9. When the first PIPS signal crosses the threshold used for coincidence determination, a 100 nsec window will be opened. At the end of this 100 nsec period, the pattern of PIPS detectors which were triggered will be compared with the logic masks. If there is a match, then 50 nsec later a second timing window for S3 opens. The S1 and S2 digitization sequence can begin at this time. After the 100 nsec S3 timing window closes, then the complete event ID is known. If this does match any of the logic masks, then a valid event has occurred and the complete data processing cycle begins. If there is no match, then the ADC is reset.

In either case, the coincidence logic is reset when the S3 window closes. Because the event processing is likely to take a relatively long time, many microseconds, there is considerable dead time. Valid coincidences will, on occasion, occur during the processing. Because the

coincidence logic is reset after 250 nsec, and the rate of true coincidences is counted by the scaler, a dead time correction can be made.

A block diagram of the anticipated design of the entire digital signal processing (DSP) electronics is shown in Figure 10. The heart of the DSP is the finite state machine (FSM). When a valid event occurs, it will 1) read the event ID, 2) look up the PIPS levels in a lookup table, 3) look up the channel number from the S1S2 table, and then update the spectrum in the current RAM buffer A, or B. The RAM buffers contain the actual output spectra. By using two buffers, data can be written into one while data are read out from the other.

The microprocessor will read the spectral data from the RAM buffer, via the FSM, and will also read the scalers, control the housekeeping ADC (HK), and output the data to the 1553 interface. The program executed by the microprocessor and the default lookup tables are stored in ROM. When new lookup tables and logic masks are sent to the instrument, the microprocessor passes them through the FSM into RAM.

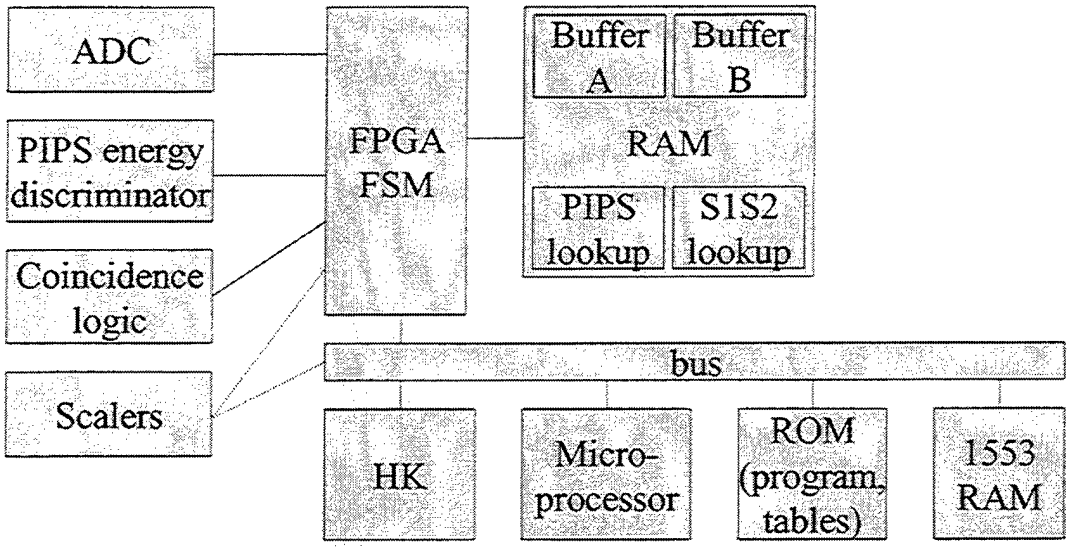

Figure 10. Block diagram of the intended architecture for signal processing in HEP.

This is the intended overall architecture for the digital electronics to be used in HEP. In the next year, considerable effort will go into preparing the detailed design and fabricating the electronics. Various aspects of this architecture may change, based on the design process.

3 HEP SENSOR HEAD RESPONSE TO PROTONS

3.1 ANALYTICAL CALCULATIONS

Average energy loss by charged particles in matter is described by the Bethe-Block equation. An extensive discussion of this equation and tabulations of stopping power, dE/dx, and range for protons in various elements and compounds is found in Ref. 1. The scintillator materials considered for use in this program are relatively new and are not listed in the Tables of Ref. 1. Therefore, some additional computation was required to obtain the needed information for these materials. As was discussed in the previous annual report, we computed the stopping power of the GSO from that of its constituent elements by the Bragg-Kleeman rule. This is only accurate to within about 10%, due to compound effects on stopping power. Research using the

EM showed that a 5% correction provides excellent agreement between the GSO data and the Bethe-Block calculations.

In order to design the sensor stack, software was written to compute the amount of energy deposited by energetic protons in each layer of a multilayer target, using the Bethe-Block approximation. The current version handles protons with energies from 100 keV to 500 MeV, up to 15 different layers, and materials containing up to five different elements. It is based upon integration of the stopping power, dE/dx, to obtain energy loss; the Janni range energy tables to determine linear stopping power for elements; and the Bragg-Kleeman rule estimating stopping power in compounds. For each of the 15 layers, the user can specify which compound is present, along with the thickness of that layer. The user also specifies the upper and lower energy bounds and the number of energy steps. The software then computes, for each incident proton energy, the amount of energy deposited in each layer. For thick layers, the deposition of energy in the various layers is computed from the change in the range of the proton. When the range of the particle is larger than ten times the thickness of a layer, an alternate method is used. In this case, the energy lost is computed as $\Delta E = (dE/dx)\ \Delta x$, where Δx is the thickness of the layer. In principle, both the dE/dx and change in range methods should give the same results, but because of numerical effects, the dE/dx method is more accurate for layer thicknesses much smaller than the range of the particle. Some outputs from this software are shown in Figures 2 and 3 of this report. This software was used to optimize detector thicknesses, to design the electronics by determining signal sizes, to design shielding, and for a wide variety of tasks.

In addition to the analytical energy loss calculations using the Bethe-Block equation, we have undertaken a series of Monte Carlo simulations of the response of the HEP sensor head to high energy protons using the LAHET code. This code follows the history of each incident proton, on an "event-by-event" basis, as it traverses the sensor head, interacting with the sensor head electrons and nuclei. This allows us to obtain extremely detailed information about the distribution of energy loss values in the sensor head detectors. This is in contrast to the Bethe-Block calculations, which result in the computation of average values only. In addition, the LAHET code realistically treats the effects of nuclear interactions in the HEP detectors.

HEP Response to Off-Axis Protons

In order to optimize the design of the collimator, shielding, and digital signal processing, software was written to compute the response of HEP to off-axis protons. The software compared a three-dimensional ray tracing subroutine, a cylindrically symmetric model of the instrument, and the multi-layer energy loss routine described above.

This software was used to determine the response of the instrument to particles incident in the collimator aperture at angles off the symmetry axis. The collimator dimensions were selected so that no out-of-aperture trajectories affect the type C events. All of the proton trajectories meeting the requirements of the type C PIPS logic and commensurate S1S2 bins are incident within the collimator opening (to within the limits of the Bethe-Block continuous-slowing down approximation). This provides for a clean measurement of the highest energy protons. The geometric factor for type C events is independent of energy and depends only on the solid angle defined by the PIPS detectors. The geometric factor for type A and B events will be energy dependent. Particles passing through D1, D2, and into S1 at large angles with respect to the symmetry axis will only have a short path length in S1, and will then strike S3. Low energy protons on such trajectories will stop in S1, and be accepted, but high energy particles

will reach S3 and be vetoed. Higher energy type A and B protons must enter over a narrower solid angle to be accepted, therefore the geometric factor for in-aperture protons will be energy dependent.

The software also computes the effects on the instrument of high energy protons which are incident near the aperture but pass through the shielding, lose energy, and then pass through the active portions of the detectors. Since the front shielding has a range of 130 MeV, protons incident above this energy will pass through the shielding. Most of the trajectories will either miss one of the detectors required for a valid coincidence, or will pass through the S3 veto. However, some trajectories will, at the proper energy, trigger the HEP logic. For example, a proton with energy only slightly exceeding the threshold may, if it is incident at the correct location and angle, pass through the shielding, pass through D1 and D2, and stop in S1. In such case a moderate energy (e.g. 150 MeV) proton will count as a lower energy (e.g. 30 MeV) proton. Higher energy protons will pass through S1 and trigger S3, and will therefore be rejected.

Software modeling was used to optimize the design of the sensor stack. The collimator material, tungsten, was chosen so that particles passing only partially through the collimator will lose as much energy as possible. The locations of the PIPS detectors were chosen to maximize the rejection of out-of-aperture protons. With the current design, if HEP is exposed to an isotropic distribution of protons with an energy spectrum given by the AP8 model at the peak of the inner radiation belt, then <1% of the measured counts for type B events will come from outside the nominal instrument aperture. For type A events in the energy channels above 80 MeV, <10% of the counts will come from outside the nominal aperture. The lowest energy type A channels, <80 MeV, will experience up to 35% of the counts from outside the nominal aperture. Fortunately, the same particle population that causes the false A events will generate a recognizable signal in the data. Specifically, particles incident at the same energy and angle to cause false A events will generate type B logic masks with type C S1S2 bins. The HEP signal processing electronics will record the rate of these background events, and return them to the ground, permitting the type A count rate to be corrected in post-flight data processing. Most of the false A events are caused by moderate energy protons (130 to 200 MeV), which stop in S1 after passing through the shielding. Most of the higher energy protons pass through S1 into S3, and are thereby vetoed.

HEP Response to In-Aperture Protons Undergoing Nuclear Interactions

A significant fraction of the protons incident on HEP will undergo inelastic (nuclear) scattering events. The energy of the incident protons measured by HEP greatly exceeds the binding energy per nucleon and Coulomb barrier for the materials in HEP. The binding energy per nucleon ranges between 7 MeV (Gd) and 23 MeV (O), while the Coulomb barriers range from 2 MeV (O) and 10 MeV (Gd). The protons measured by HEP clearly have sufficient kinetic energy to undergo inelastic nuclear scattering.

Protons undergoing inelastic nuclear scattering will deposit energy in either S1 or S2 scintillator that does not match that expected by the Bethe-Block formula, which is the basis for the nominal energy channels. This causes the instrument electronics to reject nuclear interaction events, reducing the proton flux measured in the nominal channels by the fraction of the total events that result in nuclear interactions. Background channels will be assigned with appropriate

S1S2 amplitudes and PIPS logic masks to measure nuclear interactions, to allow corrections for this effect.

The probability of a nuclear interaction may be estimated using a simple geometrical model. In order for a nuclear interaction to take place, the incident proton must overcome the repulsive Coulomb barrier, B_C, of the target nucleus and approach within a distance, R_C, where the proton comes in physical contact with the target nucleons. The geometric cross-section thus computed is the upper limit on the nuclear interaction probability, giving the number of protons which could possibly cause a nuclear reaction. As was shown in the last annual report, at the high energy limit this gives a probability of about 10% per cm in GSO. Since HEP has a total path length of 5 cm of GSO, nuclear interactions will clearly be very important. As discussed below, the actual probability of a nuclear interaction occurring in the GSO is probably closer to 20% than 50%, but this is still very important.

Nuclear interactions involving nucleons incident on complex nuclei at energies below 2 GeV can be described by assuming that the reaction proceeds by a fast cascade followed by a slower evaporation. The wavelength of the incident nucleon is smaller than the average internucleon distance, so the cascade is described in terms of particle-particle collisions within the nucleus. In the cascade, an energetic incident proton strikes a nucleon, transferring most of its kinetic energy. The nucleon may immediately exit the nucleus, or may strike other nucleons in a series of collisions. Some of these nucleons will have sufficient energy to escape the nucleus, while others will still be bound. At the conclusion of the cascade, a small number of highly energetic nucleons will have been emitted, while the residual nucleus will be in an excited state, in which no individual nucleon has sufficient kinetic energy to escape. The excited nucleus will decay to its ground state by emitting nucleons which remove the excess energy, a process called evaporation. Because of the Coulomb barrier, protons require several MeV more kinetic energy than neutrons to escape. During the cascade phase, this difference in energy is small relative to the total incident kinetic energy, so cascade protons and neutrons are emitted with equal probability. During the evaporation phase this energy difference is important, so neutrons are preferentially emitted. Some energy can be liberated due to the difference in the mass deficit of the initial and final nuclei, but this is usually small relative to the other energies involved.

The effect of these interactions on HEP are due primarily to the fact that neutrons are not detected in HEP, but will escape the sensor with whatever kinetic energy is transferred. In addition, some protons will be generated with kinetic energy lower than that of the initial incident proton, and these will have a higher dE/dx than the initial proton. A qualitative analysis of the physics, given below, will permit the selection of the proper S1S2 bins to measure nuclear interactions. A quantitative analysis of nuclear interactions requires numerical simulation. We used the LAHET Monte Carlo model, in which the nuclear interactions are described by the Bertini model discussed above.

Consider type A incident protons, which stop in S1 and therefore deposit full energy in S1. If such a proton undergoes a nuclear interaction in S1, and secondary protons are emitted, then these have short range and the full energy is still deposited in S1. If secondary neutrons are emitted, as is most likely, then less than the full energy is deposited in S1. In this case, the measurement will indicate a lower incident energy. The result is misbinning from higher to lower energies, within the type A range.

Consider now type B incident protons, which stop in S2. If such a proton undergoes a nuclear interaction in S1, and the excess energy goes into neutrons, then this will be measured as a type A (lower energy) event. If enough energy goes into protons, then more energy can be deposited in S1 than is permitted by the Bethe-Block calculation. This produces counts which appear in unique S1S2 bins, "off the end" of the S1S2 curve along the S1 axis. Some of these secondary protons may reach S3, thereby vetoing the event. If a type B proton interacts in S2 and protons are produced, then the full energy is still deposited in S2. If neutrons are produced, then the event deposits in S1 the energy expected from Bethe-Block but less energy in S2 than is expected. This produced an S1S2 signature which is below the Bethe-Block curve.

Type C incident protons may interact in S1, producing effects similar to those discussed for type B. The probability of emitting lower energy protons is higher, therefore the probability of an S3 veto is higher. Type C protons which interact in S2 may produce neutrons, depositing less energy in S2 than is expected from Bethe-Block, or may produce enough low energy protons to deposit more energy in S2 than is expected from Bethe-Block. Thus, nuclear interactions in S2 should produce a band in the S1S2 plane, with the S1 energy equal to that expected from Bethe-Block and varying S2 values, from near zero to quite large.

Figure 11 is a plot of S1S2 values, comparing those obtained using the HEP EM at the AGS, at an energy of 1.3 GeV, with simulation results at 0.5 GeV. In the measurements, a peak is visible at the point predicted by the Bethe-Block expression. The band of events with fixed S1 values and a range of S2 values is also clearly seen. This corresponds to protons passing through S1, depositing the expected energy via ionization, then undergoing a nuclear interaction in S2. In the simulation plot, the primary ionization peak is suppressed for clarity. The finite energy resolution of the scintillators is simulated by numerical peak broadening, adding a random number with gaussian distribution. The curve showing energy expected from the Bethe-Block equation is also shown.

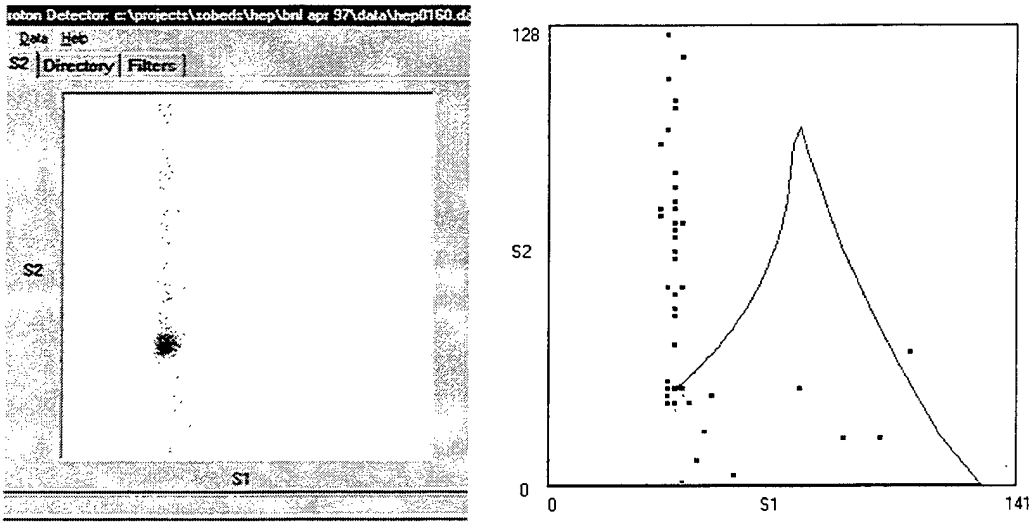

Figure 11. Scatter plots showing the pattern of (S1,S2) measured energies. The measurements (a) were obtained at 1.3 GeV at the Brookhaven AGS using the engineering model. The simulation (b) was for 520 MeV. The distribution of energies matches that expected from physical arguments and from the LAHET model.

3.2 EXPERIMENTAL SETUP

The experimental data taken in the last year used the protoflight sensor head with protoflight preamplifiers, a breadboard of the analog electronics, and external electronic modules. Custom designed modules, along with commercial NIM and CAMAC electronics, were used for data processing and acquisition. The use of external electronics permitted the work on the sensor head to proceed independently and in parallel to the work on the development of HEP digital electronics.

A block diagram of the electronics is shown in Figure 12. The goal of the electronics is to determine, on an event-by-event basis, the energy deposited in the seven detectors when a proton passed through the instrument. The primary electronic components are (1) the ADC, which digitized the analog signals corresponding to deposited energy, and (2) the coincidence circuitry, which gated the ADC when a valid event had occurred. Additional components include a scaler, to measure the actual count rates, a time-of-flight telescope, to separate protons from the lighter particles produced at Brookhaven, a monitor detector, and a motion control system. The operation of the time-of-flight telescope was described in detail in the previous annual report.

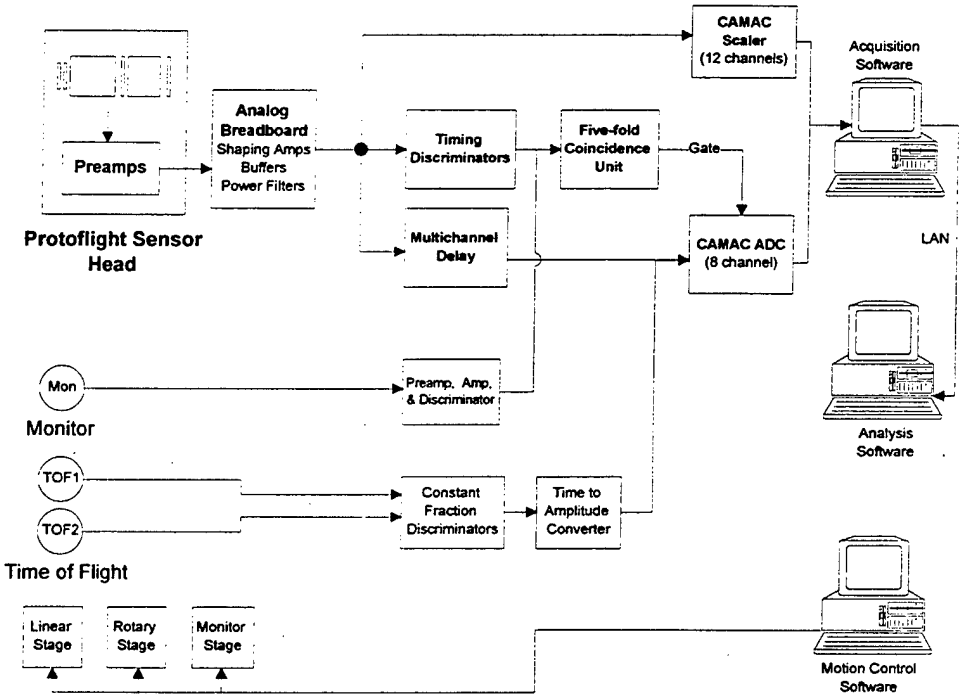

Figure 12. Block diagram of experimental set-up used to measure the HEP protoflight sensor response.

The protoflight sensor head contains, in addition to the sensors, preamplifiers and a portion of the shaping amplifier circuitry. The outputs of the sensor head were sent to a breadboard version of the analog board, containing the rest of the shaping amplifier circuitry. Because the external electronics were located outside of the beam line for personnel access, a distance of up to 100', the analog breadboard included buffer circuits, not intended for the flight boards, to drive the 100' coaxial cables.

The Analog Breadboard module produces seven shaped and amplified analog signals, proportional to the energy deposited in each of the seven detectors in the sensor head. There were five inputs to the Coincidence module, which could be selected from among D1, D2, D3, D4, a beam monitor solid state detector and a time-of-flight (TOF) telescope signal. The Coincidence Model could be configured to accept any combination of these five signals, including singles counts from any sensor, as a valid event. For a valid event, the Coincidence unit generated a logic signal which gated the CAMAC ADC. Thus, unless a preset coincidence requirement was met the ADC did not digitize any signals. Once a valid event occurred, the ADC performed pulse height analysis on all (up to eight) of its input signals. The CAMAC scaler was used to count the beam induced events in all of the sensor head detectors (S1, S2, S3, D1, D2, D3 and D4), the beam monitor detector, and the TOF telescope. In addition, the total number of valid events, as determined by the Coincidence unit, was also counted.

The HEP beam experiments were controlled by a computer network. One computer ran the data acquisition program HEPDAQ, which communicated with the CAMAC crate using a SCSI card. HEPDAQ polled the CAMAC crate for valid events accepted by the ADC. If such an event (receipt of a gate from the Coincidence unit by the AD811) occurred, HEPDAQ would 1) transfer the digitized pulse height data for that event to the computer, 2) clear the old data from the ADC and 3) enable the ADC to accept the next event. After every 250 events processed by HEPDAQ, the program would read and clear the data from the scaler.

HEPDAQ stored the data retrieved on an event-by-event basis in a disk file. In order to free up the system resources for CAMAC communications, HEPDAQ performed no data analysis and was strictly a data retrieval and storage program. A second computer ran the data analysis and display program. This program would periodically access the data file written on the data acquisition computer by HEPDAQ, using a small local area network, perform simple analysis on the data and update the various displayed spectra and scaler counts.

A third computer ran another program which communicated with the motion control system using the PC-38 card, supplied by the motion system manufacturer. The motion control system included one rotary and two linear stages. The sensor head was mounted on top of the rotary stage, which in turn was attached to a linear stage. This configuration allowed the sensor head to be moved perpendicularly to the beam and rotated with respect to the beam axis. The solid state beam monitor detector was mounted on the second, independent linear stage (the Monitor Stage). This allowed the monitor to be placed in the beam line and directly upstream of the sensor head, whenever desired by the experimenter.

3.3 Experimental Results

Amptek, Inc. staff conducted an intensive experiment at the Harvard Cyclotron during the last weekend of September, 1998. The purpose of the work was to evaluate the performance of the HEP protoflight sensor head when exposed to in-aperture proton beams with energies between 20 and 160 MeV, and to calibrate the instrument over this energy range. The protoflight sensor head, including collimation and shielding, sensors, and electronics were used, with the electronic setup described above.

The cyclotron at HCL produces a 160 MeV proton beam. The beam exits the vacuum environment of the accelerator through a thin pressure window and enters the room where the experiment is performed. Just downstream of the window, the beam is directed through a 3.2 cm

diameter collimator. Several calibrated degrader plugs (made of lead and Lexan) can be inserted into the collimator tunnel to decrease the incident beam energy. The standard degrader set produces the following mean energies at the exit of the collimator: 29, 37, 45, 54, 73, 92, 111, 131 and 149 MeV. The sensor head was located 165 cm downstream of the collimator.

A plot of the response of the instrument to the in-aperture incident protons is shown in Figure 13. In Figure 14, a spectrum measured using 110 MeV protons with the current protoflight sensor, using photodiode readouts and Spectralon reflectors, is compared with a spectrum obtained previously using photomultipliers. This shows very clearly that the sensor and electronic design planned for the flight instrument do not degrade the total resolution relative to that obtained previously. In particular, the use of the PIN photodiodes instead of photomultipliers, the use of a fast shaping time to minimize pulse pile-up, and the detector geometry and light collection techniques had no measurable impact on resolution. The signal size, electronic noise, and signal to noise ratio were as expected for all detectors, including the S3 veto scintillator. Off-axis measurements were obtained and will be compared with calculations to verify the shielding effectiveness.

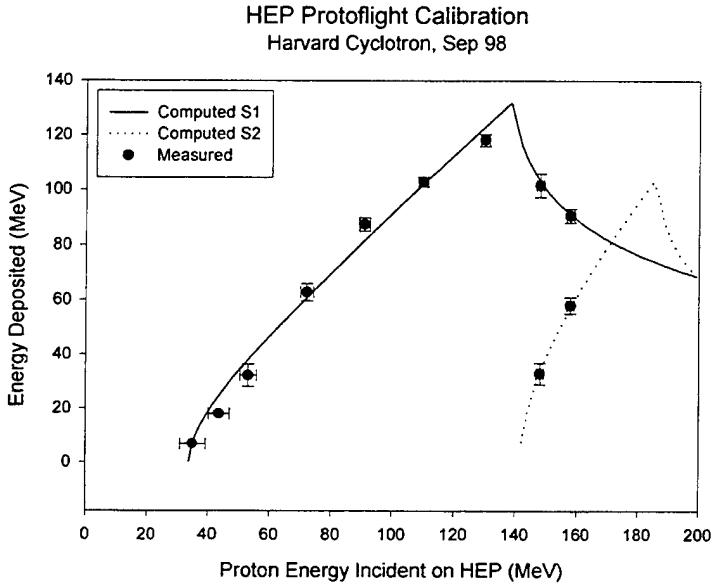

Figure 13. Plot comparing the computed response of HEP to that measured at the Harvard Cyclotron, using the protoflight sensor head, which is identical to the flight sensor head.

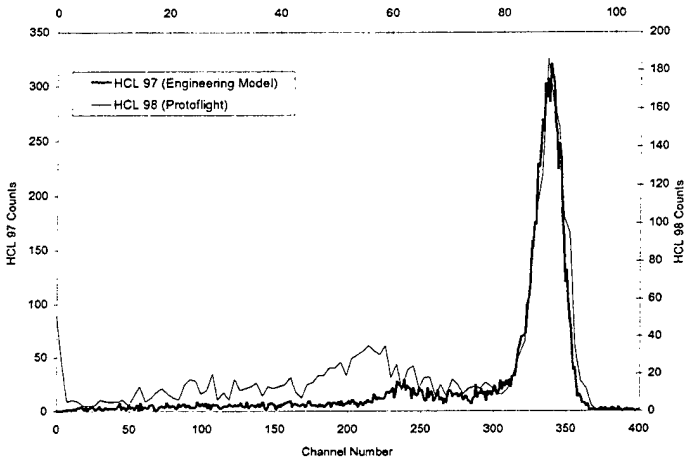

Figure 14. Spectrum generated in the S1 scintillator by 110 MeV protons, comparing the response of the protoflight unit to that obtained previously using the engineering model.

Work in this area is expected to continue into the next year. In particular, a major calibration effort is planned at the Brookhaven National Laboratory AGS accelerator during October. The response of the HEP sensor head to protons between 200 and 2,000 MeV will be measured.

4 LEPDOS DESIGN AND FABRICATION

4.1 DESIGN, FABRICATION, AND CALIBRATION OF STANDARD LEPDOS UNITS

A primary technical effort on LEPDOS in this third year of the SOBEDS contract was the design, fabrication, and testing of two flight LEPDOS instruments. We reviewed the LEPDOS instrument design and made a number of modifications to facilitate manufacturing.

One flight instrument was completely fabricated and is currently undergoing testing. It has undergone most of the functional and environmental testing. A calibration of this LEPDOS unit was performed at Goddard Space Flight Center to validate changes made to the particle telescope design. The on-board data processing algorithms in the LEPDOS unit were also checked and verified at a number of select energies during the calibration. Protons were measured from 740-1450 keV and electrons from 40-120 keV. This flight instrument is scheduled for delivery and launch in the next year of the contract.

A second flight instrument has been partially fabricated. It is identical in design to the completed unit.

4.2 DESIGN OF LEPDOS WITH ESA

A second major technical effort on LEPDOS in this third year of the SOBEDS contract has been the design of an engineering model LEPDOS instrument which includes an electrostatic analyzer (ESA) to measure electrons with energy below the threshold of the standard LEPDOS sensors. SCATHA data has indicated that spacecraft surface charging in geostationary orbit is due primarily to electrons with energies of 20 to 50 keV, with some charging due to lower energy electrons. The standard LEPDOS instruments do not directly measure the particle flux

below 50 keV, but extrapolate from higher energies. The LEPDOS with ESA will directly measure the lower energy population.

The ESA has been designed to measure electrons with energies between 500 eV and 50 keV. It will have an integrated angular response, relying on the isotropy of the electron population at geostationary altitudes for accurate measurements. It has been designed to obtain accurate measurements even at the highest observed electron fluxes. The spectral data from the ESA will be used by the LEPDOS processing algorithm to set the Surface Charging Hazard Register and associated Warning Flag. A select set of spectral data will be available in the Science Telemetry Packet and in a History Data Channel.

The ESA is a modular design, which simply attaches to the side of the existing LEPDOS instrument. Few changes are required to LEPDOS: adding a connector and some counters and control logic. All of the necessary electronics, including the HV supply, are contained within the ESA on the side. This greatly simplifies the manufacturing of both standard and enhanced instruments.

At this stage, a preliminary design has been produced. In the next year, a prototype detector will be fabricated and tested, along with the necessary electronics. Delivery of the flight unit is scheduled for next year.